Applied Ocean Research 70 (2018) 76–86

Contents lists available at ScienceDirect

Applied Ocean Research

journal homepage: www.elsevier.com/locate/apor

Sea state estimation using vessel response in dynamic positioning

Astrid H. Brodtkorb[a,*], Ulrik D. Nielsen[a,b], Asgeir J. Sørensen[a]

[a] Centre for Autonomous Marine Operations (NTNU AMOS), Department of Marine Technology, Norwegian University of Science and Technology (NTNU), NO-7491 Trondheim, Norway
[b] DTU Mechanical Engineering, Technical University of Denmark, DK-2800 Kgs. Lyngby, Denmark

ARTICLE INFO

Article history:
Received 5 May 2017
Received in revised form 17 August 2017
Accepted 13 September 2017
Available online 13 December 2017

Keywords:
Sea state estimation
Vessel response
Dynamic positioning
Closed-form expressions

ABSTRACT

This paper presents a novel method for estimating the sea state parameters based on the heave, roll and pitch response of a vessel conducting station keeping automatically by a dynamic positioning (DP) system, i.e., without forward speed. The proposed algorithm finds the wave spectrum estimate from the response measurements by iteratively solving a set of linear equations, and it is computationally efficient. The main vessel parameters are required as input. Apart from this the method is signal-based, with no assumptions on the wave spectrum shape. Performance of the proposed algorithm is demonstrated on full-scale experimental DP data of a vessel in three different sea states at head, bow quartering, beam, stern quartering and following sea waves, respectively.

1. Introduction

Complex marine operations are moving further from shore, into deeper waters, and harsher environments, see Sørensen [1]. The operating hours of a vessel are weather dependent, and good knowledge of the prevailing weather conditions may ensure cost-efficient and safe operations. In addition, the performance of the DP operation will be improved by fast dynamic tracking of the first order wave induced motions used as input to the wave filter in the DP system. Recently, there has been a lot of focus on increasing the level of autonomy in marine operations, see Ludvigsen and Sørensen [2], and having a fast and reliable method for obtaining a sea state estimate is useful both in the control and in decision support systems to aid the decision making process, with or without the operator onboard the vessel.

Several methods exist for obtaining information about the sea state. Wave rider buoys are present at fixed locations, usually near the coast, providing accurate measurements for specific sites. Some vessels have installed wave radar, see Clauss et al. [3], but these systems may be expensive to install, require frequent calibration [4,5], and in the case of large vessel motion the measurement quality is degraded. The satellite image quality may be affected if the cloud cover is low, and in general, weather data may lag up to six hours.

Today, the majority of marine vessels are equipped with sensors that gather vast amounts of data regarding the operational state, fuel consumption, hull girder stresses, acceleration, attitude and position, to name a few. In this sense, many marine vessels are inherently equipped with sea state measuring systems, since the sensor measurements can be used to infer about the on-site sea state, in a similar way as is done with traditional wave rider buoys. Estimating the sea state based on vessel motions has been explored extensively over the last 10–15 years, e.g., [6–9], see Nielsen [10] for an overview of the different methods. One proposed method is called the *wave buoy analogy*, where the ship motions in 6 degrees of freedom, or other global ship responses such as hull girder stresses, are transformed into the frequency domain, and an estimate of the wave spectrum is obtained by means of parametric or Bayesian modeling. The vessel is implicitly assumed to be in stationary conditions if not elaborate procedures are applied [11,12].

For advanced controller schemes, e.g., hybrid or switching control, sea state parameters estimated using computationally efficient algorithms are sought. In steady state DP operations, reliable and accurate estimates of the sea state are more important than frequent updates, while in transient operations (i.e., start up, change of heading and similar) fast updates even at the expense of accuracy are favoured. *Online* sea state estimates from rapid schemes, can be used to manipulate parameters in the control law directly [13], or be input to performance monitoring functions and risk assessment models that choose the best algorithms available. There are many computationally efficient schemes for estimating the peak frequency of the waves, however, algorithms for estimating the wave height and direction are rare. Belleter et al. [14] present a time-

* Corresponding author at: Centre for Autonomous Marine Operations (NTNU AMOS), Department of Marine Technology, Norwegian University of Science and Technology (NTNU), Otto Nielsens vei 10, NO-7491 Trondheim, Norway.
E-mail address: astrid.h.brodtkorb@ntnu.no (A.H. Brodtkorb).

https://doi.org/10.1016/j.apor.2017.09.005
0141-1187/

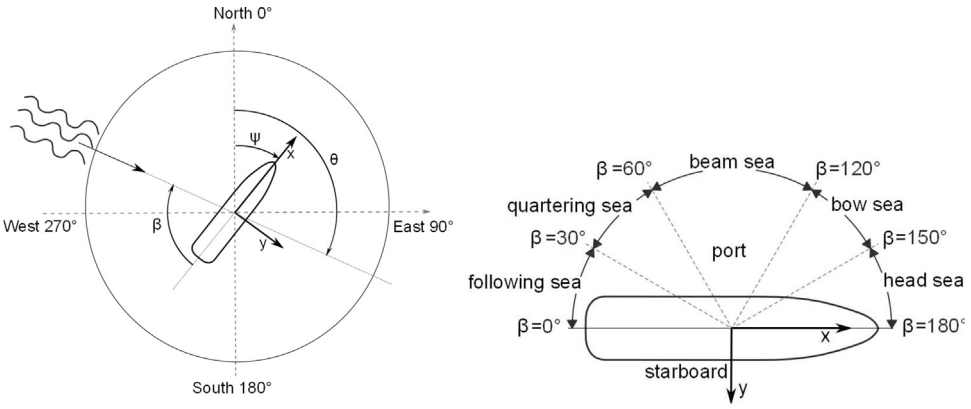

(a) Global wave propagation direction Θ (b) Relative wave direction β

Fig. 1. Definition of the wave propagation direction $\Theta \in [0, 360)^\circ$, heading of the vessel ψ, and relative wave direction β. Starboard incident waves have $\beta \in (-180, 0]^\circ$, and port incident waves have $\beta \in [0, 180]^\circ$. The coordinate system x–y represents the *body*-frame with the z-axis pointing down (into the page), and the dashed coordinate frame in (a) is the North-East-Down (NED)-frame, also with the down-axis pointing downward (into the page). Notice that the vessel is symmetric about the x-axis.

domain method for estimating the peak frequency of encounter in order to detect parametric rolling, and Brodtkorb et al. [15] use the response spectra in heave and pitch to estimate the peak frequency of the sea state for use in controllers. Nielsen et al. [16] estimate the amplitude, phase and frequency of a regular wave, making a step towards a sea state estimation algorithm that is computationally efficient, *and* provides the wave height and direction estimate, in addition to the peak frequency. On a related note, the vessel response history itself may also be used for predicting the vessel response deterministically up to 30-60 seconds ahead of time using the correlation structure in the time history process, see Nielsen et al. [17].

This paper proposes a computationally efficient and robust sea state estimation algorithm that provides an estimate of the wave spectrum, from which sea state parameters such as the significant wave height H_s, peak period T_p (or other characteristic periods), and the relative wave direction β can be derived. The sea state estimation algorithm is non-parametric, i.e., there are no assumptions on the shape of the wave spectrum, and so the sea state estimate is obtained through solving a set of linear equations relating the wave spectrum to the response measurements via (motion) transfer functions. In this initial study, the transfer functions of a barge (box-shaped vessel) called closed-form expressions, see Jensen et al. [18], with the same main parameters as the actual vessel are used in the estimation procedure. The main reason for this is to make the procedure as simple as possible, so it can be used for vessels where the detailed hull geometry is unknown or unavailable due to non-disclosure issues. For DP vendors, this will be an advantage for i.e., efficient tuning of the DP control system. If the actual transfer functions of the vessel are pre-calculated by advanced computational tools, e.g., by panel codes or strip theory, the approach will just require interpolation in a hyper-dimensional matrix, which is done in other sea state estimation algorithms. The sea state estimation algorithm is demonstrated on the heave, roll and pitch response measurements of the NTNU-owned and operated research vessel (R/V) Gunnerus during DP tests in three different sea states with head, bow quartering, beam, stern quartering and following sea waves.

The paper is organized as follows: an introduction to wave spectra, response spectra, cross spectra and closed-form expressions is given in Section 2, and Section 3 presents the sea state estimation algorithm. In Section 4 the collection and validation of the response measurements, wave elevation measurements, and tuning of the closed-form expressions is discussed, before the estimation results are presented. Section 5 concludes the paper.

2. Vessel modeling

2.1. Vessel response in irregular waves

For control design purposes, the vessel motion is usually modeled as a mass-damper-restoring system subject to the loads from current, wind, and waves. For ships in DP the thrusters will produce mean and slowly varying generalized forces in the horizontal plane to cancel those from the environment. Therefore the DP control system influences the surge, sway and yaw motion of ships, and the *heave (z), roll* (ϕ) and *pitch* (θ) motions are more suited for sea state estimation. The measurements of heave, roll and pitch are recorded in the *body*-frame, which is defined with positive x-axis pointing towards the bow, positive y-axis pointing towards starboard, and with positive z-axis pointing down, see Fig. 1b. In DP the vessel has zero or low forward speed, so that the frequency of encounter is assumed to be the same as the incident wave frequency.

In this paper, fully developed wind-generated sea states are considered. It is also assumed that the sea state is stationary in the statistical sense (statistical properties are constant), and that the waves are long-crested, with propagation direction Θ, as defined in Fig. 1a. The wave direction relative to the vessel heading is β, with $\beta = 180^\circ$ being head sea, and $\beta = 0^\circ$ being following sea, see Fig. 1b.

The relationship between the wave amplitude and the vessel response amplitude (here only heave, roll and pitch are considered) is given by the complex-valued (motion) transfer functions $X_i(\omega, \beta)$, which can be calculated using hydrodynamic software codes. The complex-valued cross-spectra $R_{ij}(\omega)$ can be calculated as:

$$R_{ij}(\omega) = X_i(\omega, \beta) X_j(\bar{\omega}, \beta) S(\omega), \tag{1}$$

where $R_{ij}(\omega)$, $i, j = \{z, \phi, \theta\}$ are the heave, roll, and pitch response spectra, $X_j(\bar{\omega}, \beta)$ is the complex conjugate of the transfer functions in heave, roll and pitch for relative wave direction β, and $S(\omega)$ is the wave spectrum. When $i = j$, $X_i(\omega, \beta) X_i(\bar{\omega}, \beta) = |X_i(\omega, \beta)|^2$, which is the amplitude of the transfer function squared. The cross spectra $R_{ij}(\omega)$ calculated from measured responses for a data set from Run 3 are shown in Fig. 2. When $i \neq j$, $R_{ij}(\omega)$ is complex-valued, and when $i = j$ the imaginary part is zero, $\mathcal{I}m(R_{ii}) = 0$. The imaginary parts of the cross spectra pairs have opposite signs, i.e., $\mathcal{I}m(R_{ij}) < 0 \Leftrightarrow \mathcal{I}m(R_{ji}) > 0$, that are dependent on the incident wave direction. This is used later to determine β.

The vessel will act as a *low-pass filter* such that small wave length λ compared to the ship length will hardly result in any response. Hence, limited information about the waves can be obtained from

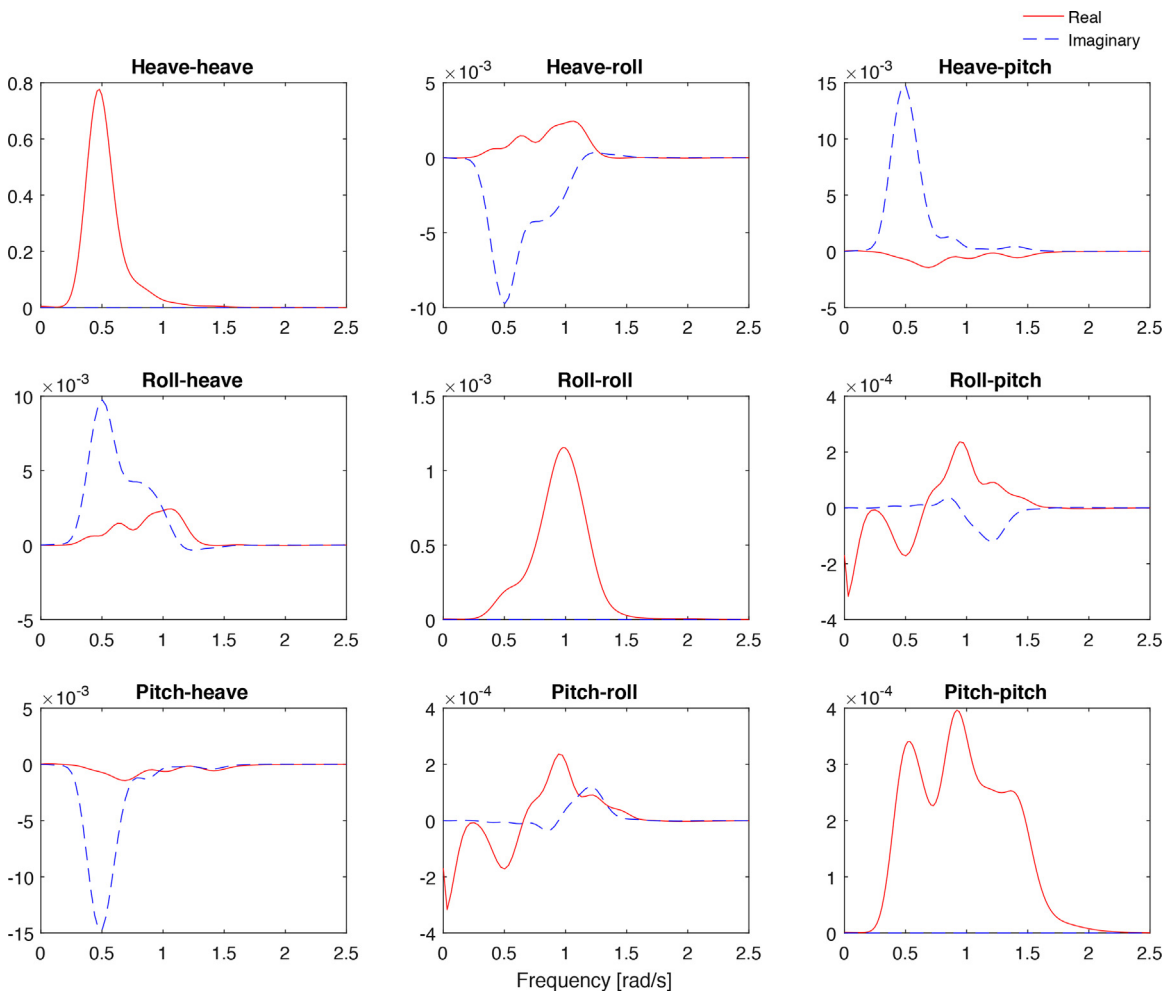

Fig. 2. Cross spectra R_{ij} calculated from measured responses in heave, roll and pitch for the data set from Run 3, head seas (see Tables 2 and 3). Frequency [rad/s] on all x-axes.

the vessel motion measurements in these cases.[1] Due to the low-pass characteristics, the algorithm will work best for wave length larger than a certain value compared to the ship length and breadth, dependent on the wave direction relatively to the vessel. For many operations, detailed information about the sea state is in particular of interest for H_s larger that 2–3 m as you get closer to the limitations for e.g., crane operations, off-loading, anchor handling, etc. The procedure implicitly assumes that the wave-induced motions are small so that linear theory is applicable though reasonable good results are obtained for higher sea states. It is also assumed that the vessel response is in steady state, though this may be relaxed, see for instance [11].

2.2. Closed-form expressions

In order to calculate the transfer functions, $X_i(\omega, \beta)$, from the wave amplitude to the response amplitude, of a marine vessel, generally a detailed description of the vessel hull geometry, weight distribution, draught and trim are required for standard as well as advanced computational tools, e.g., the 3D panel code WAMIT [19], or the 2D strip theory code ShipX [20]. In these software codes, the transfer functions are calculated for a pre-specified set of headings, loading conditions and vessel forward speeds (though here only zero forward speed is considered). Jensen et al. [18] present simplified expressions, called closed-form expressions, for the heave, roll and pitch motions of a homogeneously loaded box-shaped vessel with dimensions $L \times B \times T$ (length, breadth, draught), which approximate the transfer functions of a ship. The main reasons for using the closed-form expressions in this procedure, instead of the actual transfer functions of the ship, are:

- To demonstrate that it is possible to obtain a sea state estimate including significant wave height, a characteristic period and direction by using limited knowledge of the vessel hull geometry.
- The use of closed-form expressions offer a convenient way to deal with transfer functions in varying operational conditions without the need to interpolate.

The closed-form expressions for heave and pitch in Jensen et al. [18] are derived based on the decoupled heave and pitch dynamics of the vessel. This leads to a semi-analytical expression for the transfer functions with inputs L, B, T, block coefficient C_B, and ship forward speed V (although V is set to zero here). For roll, the closed-form expression requires the displacement Δ, water-plane area coefficient C_{WP}, transverse metacentric height GM_T, and roll natural period T_{4n} as additional input. The parameters GM_T and Δ are calculated by ballast programs onboard vessels, usually before the vessel leaves port, in order to ensure sufficient stability of the ves-

[1] Some studies look at the possibility to infer knowledge about higher frequency wave components by considering the motion of a fixed point on the ship hull relative to the sea surface by installing, for instance, a downward-looking microwave sensor; see e.g., Nielsen [31,32].

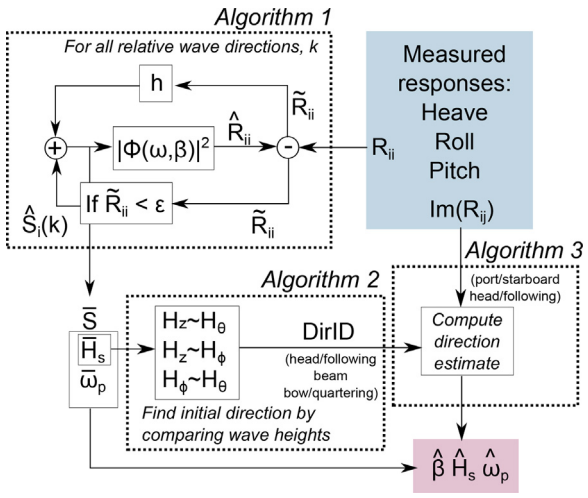

Fig. 3. Illustration of the proposed sea state estimation method, in two main steps. Firstly the point-wise wave spectrum estimate matrix $\bar{S}$ is computed by solving (4) through iteration. Secondly, the significant wave heights $\bar{H}_s$ for each of the wave spectra in $\bar{S}$ are compared to find an initial direction α, and the imaginary parts of the cross-spectra $R_{ij}(\omega)$ are used to find the relative direction estimate $\hat{\beta}$. The inputs to the procedure are the measured response spectra in heave, roll, and pitch, and the outputs are estimates of the relative wave direction $\hat{\beta}$, significant wave height $\hat{H}_s$, peak period $\hat{\omega}_p$, and the wave spectra $\hat{S}_i(\omega, \hat{\beta})$.

sel and avoid capsize. C_{WP} and C_B can be approximated for different hull shapes, and the roll natural period may be approximated by

$$T_{4n} = \frac{2\pi}{\omega_{4n}}, \quad \omega_{4n} = \frac{\sqrt{gGM_T}}{r_x}, \tag{2}$$

where g is the acceleration due to gravity, and the roll radius of gyration used here is $r_x = 0.4B$, see Papanikolaou et al. [21]. Other values of the radius of gyration may also be used.

The roll damping is important to estimate correctly, and is approximated by a linear wave-induced part, and a viscous part. In [18], the linear wave-induced damping is calculated by using two boxes that are rigidly joined, however, here only one box with dimensions $L \times B \times T$ yielded better results. The sectional damping coefficient is determined by an approximation based on the ratio B/T for a wedge-shaped hull, and then multiplied with the length L of the hull. Viscous roll damping is approximated by a factor $0 < \mu \ll 1$ of the critical damping $B^*_{44} = \frac{T_{4n} C_{44}}{\pi}$, where $C_{44} = g\Delta GM_T$ is the roll restoring coefficient. The viscous damping is highly non-linear, but linearized approximations based on the critical damping are often used both in simplified approaches, and in panel and strip theory codes. The closed-form expressions in heave, roll and pitch are in the rest of the paper referred to by $\Phi_i(\omega, \beta)$, $i = \{z, \phi, \theta\}$.

3. Sea state estimation algorithm

The sea state estimate, consisting of a wave direction estimate and a point-wise wave spectrum estimate, is computed in two main steps, as illustrated by Fig. 3. They are described in detail subsequently, but summarized as follows: Firstly, the response spectra in heave, roll and pitch, when $i = j$ $R_{ii}(\omega)$, and the closed-form expressions are used to find an initial estimate of the unknown wave spectrum $S(\omega)$. This is done by solving the following equation through iteration

$$R_{ii}(\omega) = |\Phi_i(\omega, \beta)|^2 S(\omega), \tag{3}$$

which is the relation between the sea state and the vessel response in (1) when $i = j$, $i = \{z, \phi, \theta\}$, with the transfer functions substituted with the closed-form expressions from Section 2.2. $R_{ii}(\omega)$ is the real part of the Fourier transformation of the measured heave, roll and pitch vessel response, respectively.

Secondly, the significant wave heights, computed for each degree of freedom, and for each wave direction are used to find an initial direction estimate. The imaginary parts of the cross spectra $R_{ij}(\omega)$, $i \neq j$ are used to estimate the relative wave direction $\hat{\beta}$, and then the estimates of the peak wave period $\hat{T}_p := \frac{2\pi}{\hat{\omega}_p}$ and significant wave height $\hat{H}_s$ are found.

3.1. Wave spectrum estimate

At first sight, the most obvious method to obtain the wave spectrum estimate is to invert (3). However, because $\Phi_i(\omega, \beta)$, especially for roll and pitch, are small for a large range of frequencies, the inverse squared for the corresponding frequency range is very large. As a result, solving (3) by inversion may be numerically unstable for certain combinations of frequency and directions [22–24]. In order to circumvent an ill-conditioned system with numerical instabilities, the estimation procedure proposed here is based on the solution of the linear equation (3) using an iterative scheme.

Firstly, the frequencies and directions are discretized into N_ω and N_β parts, respectively, and the discretized direction k, is used to denote directions in the estimation procedure. Since the wave direction is unknown initially, the point-wise wave spectrum estimate needs to be calculated for every direction $k = \{0, \ldots, 180\}$, and hence the estimated wave spectrum is dependent on the direction as well as frequency, $\hat{S}_i(\omega, k)$. The method does not assume a wave spectrum shape, or parametrize it in any way, and hence the initial wave spectrum estimate and estimate of the response spectrum are set to zero, $\hat{S}_i(\omega, k) = 0$ and $\hat{R}_{ii}(\omega, k) = 0$. For each degree of freedom $i = \{z, \phi, \theta\}$ and for each direction $k = \{0, \ldots, 180\}$, repeat the following steps,

$$\tilde{R}_{ii}(\omega, k) = R_{ii}(\omega) - \hat{R}^-_{ii}(\omega, k) \tag{4a}$$

$$\hat{S}_i(\omega, k) = \hat{S}_i(\omega, k) + h\tilde{R}_{ii}(\omega, k) \tag{4b}$$

$$\hat{R}_{ii}(\omega, k) = |\Phi_i(\omega, k)|^2 \hat{S}_i(\omega, k), \tag{4c}$$

until a threshold is reached $|\tilde{R}_{ii}(\omega, k)| \leq \epsilon_i$, for $\epsilon_i > 0$. In (4a), the response spectrum estimation error $\tilde{R}_{ii}(\omega, k)$ is computed by making use of the estimated response spectra from the previous iterate, denoted by $\hat{R}^-_{ii}(\omega, k)$, and the measured response spectra $R_{ii}(\omega)$. In (4b), $\tilde{R}_{ii}(\omega, k)$ is used to make adjustments to the estimated wave spectrum $\hat{S}_i(\omega, k)$, with a small step size $h > 0$, and in (4c) a new response spectrum estimate $\hat{R}_{ii}(\omega, k)$ is calculated. Note that since the transfer functions of a box-shaped vessel are applied, the values for pitch beam seas and for roll in head and following seas are zero $\Phi_i(\omega, k) = 0$. The iteration is terminated in these cases, giving a wave spectrum estimate of zero, $\hat{S}_i(\omega, k) = 0$

In summary, (4a–c) are one iteration step, which are repeated untill $|\tilde{R}_{ii}(\omega, k)| \leq \epsilon_i$, for $\epsilon_i > 0$. This is done for all degrees of freedom $i = \{z, \phi, \theta\}$ and directions $k = \{0, \ldots, 180\}$. The output from (4) are three point-wise wave spectrum estimates per direction, yielding a spectrum estimate matrix of dimension $3 \times N_\omega \times N_\beta$.

$$\bar{S} = \begin{bmatrix} \hat{S}_z(\omega, 0) & \ldots & \hat{S}_z(\omega, k) & \ldots & \hat{S}_z(\omega, 180) \\ \hat{S}_\phi(\omega, 0) & \ldots & \hat{S}_\phi(\omega, k) & \ldots & \hat{S}_\phi(\omega, 180) \\ \hat{S}_\theta(\omega, 0) & \ldots & \hat{S}_\theta(\omega, k) & \ldots & \hat{S}_\theta(\omega, 180) \end{bmatrix} \tag{5}$$

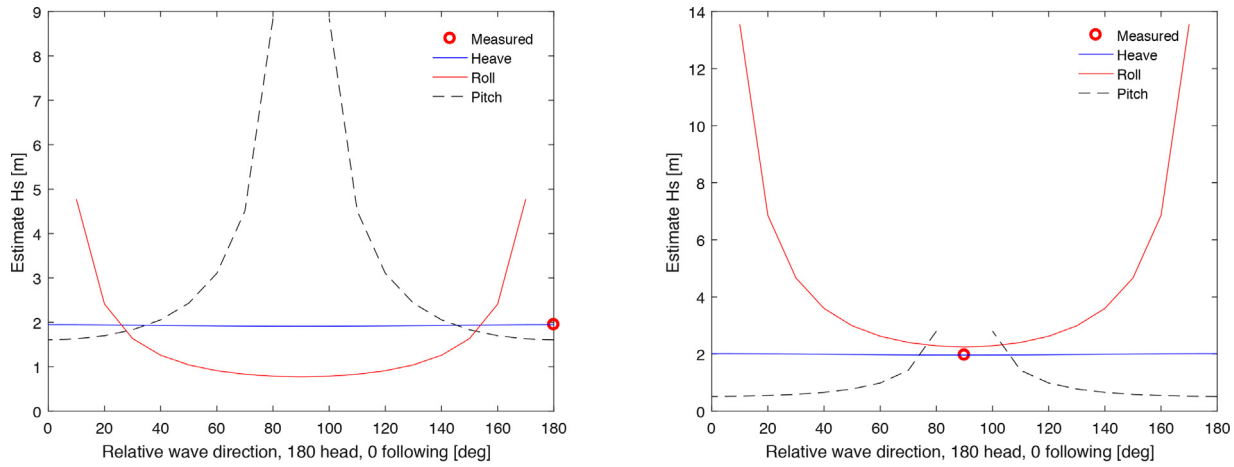

Fig. 4. Significant wave height in (6) plotted against relative wave direction. This data set is from Run 3, for actual vessel heading **head** in (a) and **beam** in (b), see Tables 2 and 3 for details. The measured significant wave height and correct relative direction are indicated by the circles.

Now it remains in this former part to compute the peak frequency and significant wave height for each of the wave spectra in $\bar{S}$. The result is collected in two matrices with dimensions $3 \times N_\beta$.

$$\bar{H}_s = \begin{bmatrix} H_z(0) & \dots & H_z(k) & \dots & H_z(180) \\ H_\phi(0) & \dots & H_\phi(k) & \dots & H_\phi(180) \\ H_\theta(0) & \dots & H_\theta(k) & \dots & H_\theta(180) \end{bmatrix} \tag{6}$$

$$\bar{\omega}_p = \begin{bmatrix} \omega_z(0) & \dots & \omega_z(k) & \dots & \omega_z(180) \\ \omega_\phi(0) & \dots & \omega_\phi(k) & \dots & \omega_\phi(180) \\ \omega_\theta(0) & \dots & \omega_\theta(k) & \dots & \omega_\theta(180) \end{bmatrix} \tag{7}$$

The iteration (4) is a set of $3 \times N_\beta$ linear equations that are computationally efficient to solve. In this paper we have used $N_\beta = 19$ directions, $k = \{0, 10, \dots, 180\}$, and $N_\omega = 300$. In the following it is explained how to make the selection of the relative wave direction estimate, considering also the interval $\beta = (-180, 0]$.

3.2. Wave direction estimate

The relative wave direction estimate is found in two stages, as indicated in Fig. 3. The initial direction α is found by using the significant wave height matrix $\bar{H}_s$ in (6), and this information is coupled with the imaginary parts of the cross spectra in heave-roll and heave-pitch. The approach for selecting the wave direction is explained in the following.

Stage A: An initial relative wave direction estimate α can be made as either *head/following*, *bow/stern quartering*, or *beam* seas by comparing how much energy is in the different wave spectrum estimates $\bar{S}$, i.e., comparing the elements of $\bar{H}_s$. In Fig. 4 the significant wave heights $\bar{H}_s$ from (6) are plotted for the same sea state (Run 3, see Table 3 in Section 4). The vessel is in head seas in (a) and beam seas in (b). The measured significant wave height and correct relative direction are indicated by the circle in both plots. The wave height estimates $H_\phi(k = 0)$, $H_\phi(k = 180)$ and $H_\theta(k = 90)$ are not included in the plots, since the closed-form expressions are zero in these cases, and the corresponding wave spectrum estimates are set to zero as well.

The estimated significant wave heights from using the heave response and heave closed-form expression vary little over the wave direction, and are close to the measured H_s, see the red dots in Fig. 4. This is used as the base case for determining the incident direction of the waves. Since the closed-form expressions for roll and pitch vary a lot over wave direction, the corresponding H_ϕ and H_θ also vary a lot with direction. The angle k where the $\bar{H}_s$ are closest, is chosen as the initial direction α, in the following way:

- $\alpha = 45$: When the sea state is bow or stern quartering, the maximum H_θ and H_ϕ are about the same order of magnitude.
- $\alpha = 0$: When the significant wave height from using pitch for head (or following) $H_\theta(k = 180)$ sea is close to the significant wave height estimate from heave for head (or following) sea $H_z(k = 180)$, the direction is either head or following. From Fig. 4a it is ruled out that the waves are approaching from the side, since then $H_\theta(k = 80)$ and $H_\theta(k = 100)$ are a lot larger than H_z for the same directions.
- $\alpha = 90$: When the significant wave height using roll in beam sea $H_\phi(k = 90)$ and using heave $H_z(k = 90)$ are close, the sea state is beam sea. In Fig. 4b, H_ϕ for $k = 10^\circ$ and $k = 170^\circ$ are significantly larger than H_z for the same directions, which rules out that the waves are head or following.

In the ideal case, using the actual transfer functions of the ship, the three significant wave height curves in Fig. 4 should cross at the same point, and this point should be the actual relative wave direction. However, since the closed-form expressions are used here, the curves are head/following and port/starboard symmetric, and an extra stage is needed.

Stage B: The next stage is to calculate the wave direction estimate $\tilde{\beta}$ by using the initial direction α from Stage 1, and the imaginary parts of the heave-pitch and heave-roll cross spectra $\mathcal{I}m(R_{z\phi})$, and $\mathcal{I}m(R_{z\theta})$. The heave response is *symmetric* about the *x*-axis (body-frame), and the pitch response is *anti-symmetric* about the y-axis, see Fig. 5 for an illustration. The symmetric and anti-symmetric properties of the responses, are reflected in the imaginary part of the heave-pitch cross spectra $\mathcal{I}m(R_{z\theta})$, which has opposite sign for head and following sea. The 'peak' of the imaginary spectra are found by

$$\begin{aligned} \text{peak}(\mathcal{I}m(R_{ii})) := \; & \{\mathcal{I}m(R_{ii}(\omega_J)) : \\ \omega_J = \; & arg\ \max_j |\mathcal{I}m(R_{ii}(\omega_j))|, i = \{z, \phi, \theta\}\}, \end{aligned} \tag{8}$$

corresponding to the largest extreme, either maxima or minima. This means that if $\text{peak}(\mathcal{I}m(R_{z\theta})) > 0$, then the vessel is in head sea,

and $\hat{\beta} = 180$, and conversely if peak($\mathcal{I}m(R_{z\theta})$) < 0, then the vessel is in following sea, and $\hat{\beta} = 0$.

For beam seas, α==90, starboard and port seas can be distinguished by using the imaginary part of the heave-roll (or roll-heave) cross spectra $\mathcal{I}m(R_{z\phi})$ in a similar manner. The roll response is *anti-symmetric* about the body x-axis, giving opposite sign for the roll angle when a wave crest approaches from port and starboard side, and the heave response is symmetric about the x-axis. If peak($\mathcal{I}m(R_{z\phi})$) > 0 then the vessel is in starboard beam sea and $\hat{\beta} = -90$, and the opposite for port beam sea. When α==45, indicating bow quartering or stern quartering seas, there are four possibilities for the wave direction, because of zero forward-speed and a box-shaped vessel. Then $\mathcal{I}m(R_{z\theta})$ and $\mathcal{I}m(R_{z\phi})$ are used in combination.

It should be realized that the outlined procedure for the wave direction estimate strictly holds only in case of zero-forward speed and for a sea state described by long-crested waves. Without forward speed, waves that are following, will always be *following*, since the vessel will not travel faster than the waves, as can happen in some cases with forward speed. The (geographical) wave propagation direction estimate $\hat{\Theta}$ can be computed by using the heading of the vessel, see Fig. 1a.

3.3. Peak frequency and significant wave height estimates

In Brodtkorb et al. [15], it was found through a series of model-scale experiments at zero forward speed, that the best peak wave frequency estimate was achieved by using the mean of the heave and pitch response peak frequencies. Therefore the mean of the peak frequencies following from the wave spectrum estimate for heave and pitch, for the estimated incident wave direction, are used:

$$\hat{\omega}_p = \frac{\omega_z(\hat{\beta}) + \omega_\theta(\hat{\beta})}{2} \tag{9}$$

The peak frequencies for the estimated wave spectrum were found to be consistent for all directions, and therefore if the wave direction estimate is not found reliable, a peak frequency estimate may still be obtained as the average of the peak frequencies obtained for all directions in heave and pitch. The peak period estimate is $\hat{T}_p = \frac{2\pi}{\hat{\omega}_p}$. In beam seas only the heave estimate is used, since the pitch estimate is set to zero.

The estimate of the significant wave height in heave is consistent for all directions, see Fig. 4, and therefore

$$\hat{H}_s = H_z(\hat{\beta}). \tag{10}$$

Again, if the wave direction estimate is not found, the average of the heave significant wave heights can be used instead.

4. Data validation, estimation results and discussion

In this section the data collection setup is described, and the data and closed-form expressions are validated before the estimation results are presented and discussed.

4.1. Data collection

The full-scale DP response measurements were collected during a test campaign in 2013 conducting DP operations of R/V Gunnerus, see Table 1 for main dimensions. The tests were originally done in order to document the effect of a thruster retrofit, where the main propulsion was changed from two conventional fixed pitch propeller-rudder combinations to two Rolls Royce rim-driven azimuthing thrusters, see Steen et al. [25]. The R/V Gunnerus is a test platform for biologists, archeologists, marine robotics, and recently for DP and autopilot algorithms [26].

Table 1
R/V Gunnerus main parameters used to calculate closed-form expressions.

Parameter	Value
Length, L_{pp}	28.9 m
Breadth, B	9.6 m
Draught, T	2.7 m
Block coefficient, C_B	0.56 [–]
Waterplane coefficient, C_{WP}	0.837 [–]
Displacement, Δ	417 000 kg
Transverse metacentric height, GM_T	2.663 m

Table 2
Summary of the test cases for Run 1–3.

Run	Relative direction β [deg]
1	{0, 45, 90, 180}
2/2*	{0, 45, 90, 135, 180}
3	{90, 180}

Table 3
Summary of sea states, with most prominent values for the significant wave height H_s, peak period T_p, wave propagation direction Θ, and direction spread, as derived from the wave buoy measurements.

Run	H_s [m]	T_p [s]	Θ [deg]	Spread [deg]
1	2.27	10	160	34.0
2	{1.1, 0.9}	{8, 13.5}	{190.2, 72}	{5.3, 10.2}
2*	1.71	8	190.2	5.3
3	1.92	15.3	72	12.4

Table 2 gives an overview over the test cases in three sea states. In the first sea state response data for head, beam, stern quartering and following sea were recorded. The second sea state has measurements for bow quartering sea as well. The third sea state only has two relative directions measured; head and beam seas. The relative directions stated here are the *intentional relative directions*, and are not exactly what was run, since the incident wave direction was judged by sight during the tests. The actual relative directions calculated from the wave buoy direction measurement and the heading of the vessel, are given together with the estimation results in Table 4. The response of the vessel was recorded for 15 minutes in each relative wave direction.

As external information, useful for validation purposes, the sea surface elevation was measured using a directional wave rider buoy that was deployed close to where the DP tests took place. The sea states are in the next sections referred to by run numbers defined in Table 3. The statistical values listed in the table are calculated from the post-processed time series from the wave buoy. The wave elevation time series used to calculate the sea state parameters correspond to the time of the DP tests for the three days. The WAFO toolbox [27] for Matlab® was used to post-process the response and wave measurements.

The sea states in Run 1 and 3 are single-peaked that resemble JONSWAP[2] spectra, and the sea state in Run 2 is double peaked like the Torsethaugen spectrum, with the first values for Run 2 in Table 3 corresponding to wind-generated waves, and the second corresponding to swell. Since the sea state estimation algorithm does not differentiate between multiple peaked spectra at this point, Run 2 is formulated alternatively as Run 2*. The peak period, direction and spread are taken as the values for the highest peak, corresponding to the wind-generated waves. The alternative formulation 2* is used in the discussion of the results. In literature, there exists

[2] Joint North Sea Wave Project

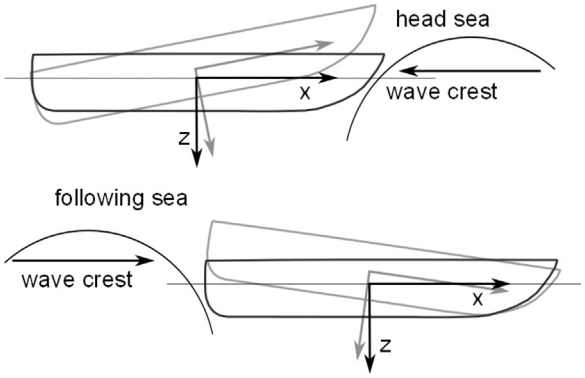

Fig. 5. Sketch of the heave and pitch responses to a wave crest for head and following sea for zero forward speed. For head sea, the heave response is upwards, with the bow upwards, and for following sea the heave response is still upwards, but not the bow goes downwards.

schemes for partitioning the wave spectra into wind-generated waves and swell, see for instance Montazeri et al. [28].

4.2. Tuning and validation of closed-form expressions

In this section the closed-form expressions are compared with the ShipX-calculated transfer functions for R/V Gunnerus. Fig. 6 compares the transfer functions calculated using ShipX and the closed-form expressions for the tuning found in this section, for encounter directions $\beta = \{90, 100, \ldots, 180\}^\circ$. The arrow indicates how the amplitude of the transfer functions vary with increasing β. A note of caution worth mentioning is that ShipX uses strip theory to calculate the transfer functions of a vessel. Since R/V Gunnerus has $L/B = 3$, strip theory is not strictly speaking valid for this vessel, however, it is considered accurate enough for validation of the closed-form expressions.

Starting with the heave and pitch closed-form expressions. In [18] it is recommended that for block coefficient $C_B < 1$ use BC_B as the breadth of the box, so that the buoyancy of the box and the ship are equal. In this case if the length $L = C_B L_{pp}$ is used instead, both the heave and pitch closed-form expressions are a lot closer to the ShipX transfer functions, and the buoyancy for the ship and the box are still equal. A reason why $L = C_B L_{pp}$ works well may be that R/V Gunnerus is a relatively short vessel compared to its breadth $L/B = 3$,

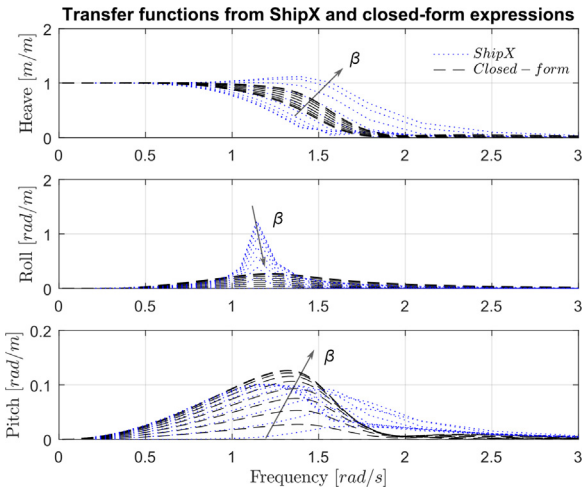

Fig. 6. Amplitudes of the ShipX-calculated transfer functions and closed-form expressions in heave, roll and pitch for $\beta \in [90, 180]^\circ$. The arrow indicates how the amplitude varies with increasing β.

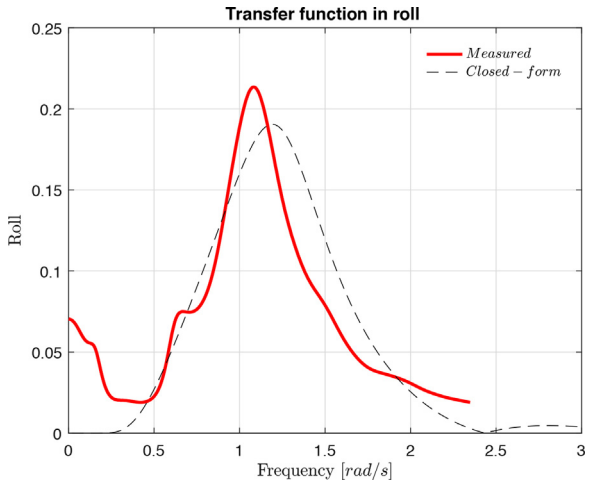

Fig. 7. Amplitude of the closed-form expression for roll compared with the *measured* transfer function for Run 2, $\beta = 45^\circ$ (stern quartering sea).

and at the same time it nearly fills a rectangle seen from above, with waterplane area coefficient $C_{WP} = 0.837$.

The roll closed-form expression needs some more attention than the others, because in general, roll is a response that is typically susceptible to larger inaccuracies due to effect of nonlinearities in damping and restoring forces. The roll response of the vessel is centred close to the roll natural frequency, with the level of damping deciding how narrow-peaked the transfer function is. Therefore the measured roll response in one sea state and one heading is used as a tuning case for the roll closed-form expression. The *measured* roll transfer function can be calculated by solving (1) with $i = j$ for the transfer function, $X_\phi^{meas}(\omega, \beta)$. The measured transfer function for Run 2 with $\beta = 45^\circ$ (stern quartering sea) is plotted alongside the amplitude of the closed-form expression in roll in Fig. 7. The roll damping and peak frequency were tuned to get similar shapes for the closed-form expression and the measured transfer function.

The sectional wave radiation damping coefficient was found using the wedge hull form, see Jensen et al. [18], as the approximations are in the correct B/T-range (B/T for Gunnerus is $9.6/2.7 = 3.55$). Adding viscous damping of $\mu = 0.3$ of the critical damping made the closed-form expression in roll similar to the measured transfer function. The viscous effects in the ShipX-calculated roll transfer function are underestimated, as seen in Fig. 6, since the peak is much higher than the roll closed-form expression. The natural frequency in the roll closed-form expression was approximated by (2) with the GM_T given in Table 1, and the radius of gyration $r_x = 0.4B$, as suggested in [21].

4.3. Data validation

In this section the data gathered by the wave buoy and transfer functions calculated using ShipX are used to validate the closed-form expressions against the measurements of heave, roll and pitch. Notice that this is the reverse process to estimating the sea state, and is only done for validation purposes. The theoretical response is calculated as follows:

$$R_{ii}^{ShipX}(\omega) = |X_i(\omega, \beta)|^2 S_{buoy}(\omega) \tag{11}$$

$$R_{ii}^{CF}(\omega) = |\Phi_i(\omega, \beta)|^2 S_{buoy}(\omega), \tag{12}$$

where R_{ii}^{ShipX}, and R_{ii}^{CF} $i = \{z, \phi, \theta\}$ are the calculated response spectrum in heave, roll and pitch, $X_i(\omega, \beta)$ are the transfer functions calculated using ShipX, $\Phi_i(\omega, \beta)$ are the closed-form expressions, and $S_{buoy}(\omega)$ is the Fourier transform of the wave elevation measured by the wave rider buoy. The direction from the buoy and the

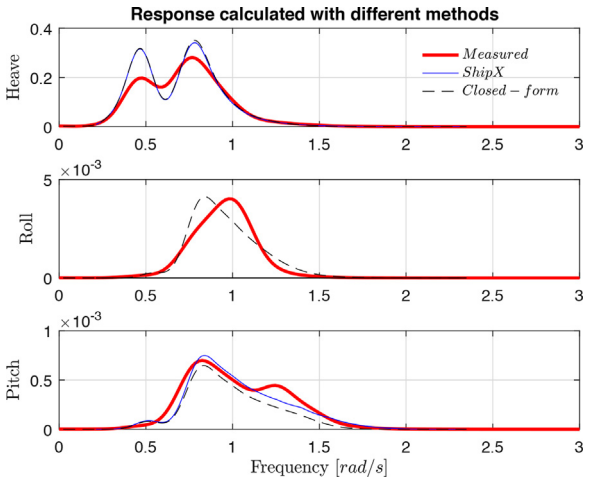

Fig. 8. Measured and calculated response spectra using ShipX calculated transfer functions and using the closed-form expressions in Section 2.2. The waves used are Run 2 for 45° (stern quartering sea).

heading of the vessel are used to calculate the relative wave direction β. Fig. 8 shows the measured and calculated response in heave, roll and pitch for Run 2, for $\beta = 45°$ (stern quartering sea).

The theoretical R_{ii}^{ShipX}, and R_{ii}^{CF}, and measured responses generally correspond well, for heave and pitch. For roll the ShipX transfer functions are overestimated (see Fig. 7), and therefore the $R_{\phi\phi}^{ShipX}$ is a lot larger than the others, and is omitted in the plot. The roll closed-form expression performs adequately. It is observed that for beam seas the measured pitch response is generally larger than the theoretical R_{ii}^{CF}, and the same goes for the roll response for close to head and following seas. One reason for this might be that the waves were not completely long-crested since the wave propagation direction had a spread, and waves with different directions than the mean wave direction excite the vessel response.

4.4. Estimation results

The procedure described in Section 3 was applied to all the response measurements available, see Table 2. Figs. 9–11 show the estimated wave spectra using the heave and pitch responses for all response time series in each sea state.

A summary of the estimated sea state parameters $\hat{H}_s$, $\hat{T}_p$ and $\hat{\beta}$ and the estimation errors are shown in Table 4. The estimation errors are calculated as

$$\tilde{\beta} = |\beta - \hat{\beta}| \quad [^\circ] \tag{13a}$$

$$\tilde{H}_s = 100\frac{|H_s - \hat{H}_s|}{H_s} \quad [\%] \tag{13b}$$

$$\tilde{T}_p = 100\frac{|T_p - \hat{T}_p|}{T_p} \quad [\%], \tag{13c}$$

with β, H_s and T_p calculated from the wave buoy measurements, see Table 3. Note that the pitch response is zero for beam seas, so no sea state estimate from pitch is obtained for this direction. Inherently, the estimates are in the *encounter domain*, but since the forward speed is zero, this is equivalent to the true domain.

From examining the Figs. 9–11, it is observed that generally the estimated wave spectrum based on the heave response is closer to the measured wave spectrum than what the pitch estimates are. The pitch estimate is generally the best when the relative wave direction is bow quartering or following sea. For the estimates in stern quartering sea for Run 1 and 3, and for head sea in Run 3, the pitch response underestimates the peak of the wave spectrum a lot, probably since the approximation of the bow quartering as a box-shape is not accurate. Using the heave estimate for computing the significant wave height yields consistent results, with a mean estimation error for wave height of $\tilde{H}_s = 5.79\%$ over all directions, with a standard deviation of 3.78%. The largest estimation error is $\tilde{H}_s = 12\%$, which occurs in Run 1 for stern quartering seas.

For the two-peaked spectrum, Run 2 in Fig. 10, the heave response is double-peaked for all the directional estimates,

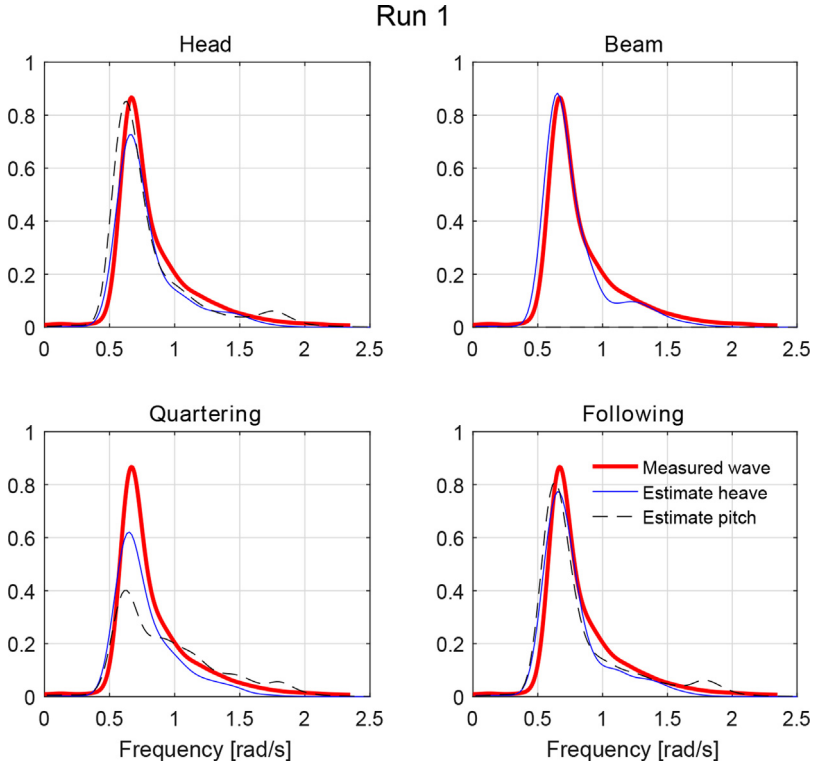

Fig. 9. Measured and estimated wave spectra [m^2 s] using the heave and pitch response; $S(\omega)$, $\hat{S}_z(\omega, \hat{\beta})$, and $\hat{S}_\theta(\omega, \hat{\beta})$, for the sea state in Run 1.

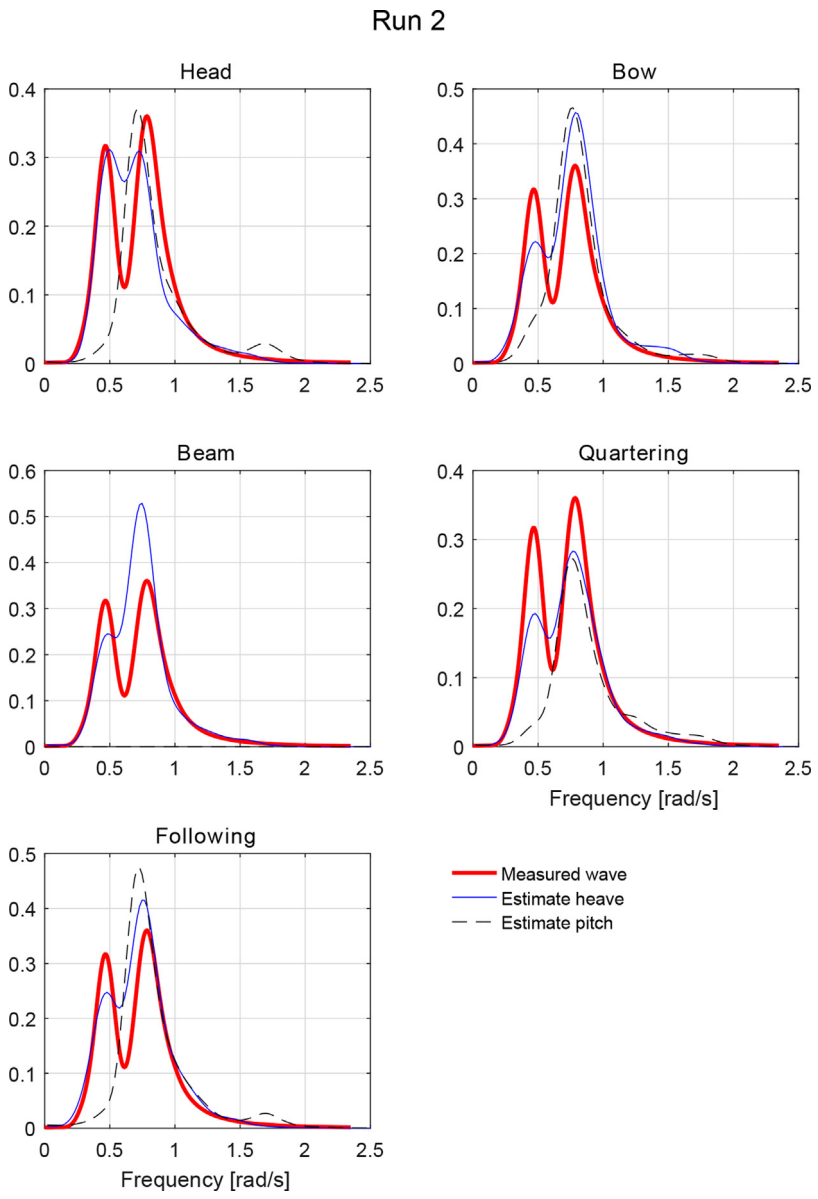

Fig. 10. Measured and estimated wave spectra [m^2 s] using the heave and pitch response; $S(\omega)$, $\hat{S}_z(\omega, \hat{\beta})$, and $\hat{S}_\theta(\omega, \hat{\beta})$, for the sea state in Run 2.

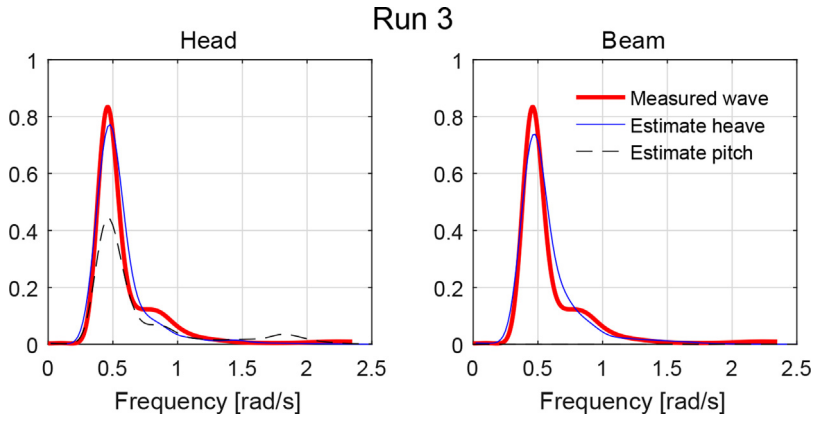

Fig. 11. Measured and estimated wave spectra [m^2 s] using the heave and pitch response; $S(\omega)$, $\hat{S}_z(\omega, \hat{\beta})$, and $\hat{S}_\theta(\omega, \hat{\beta})$, for the sea state in Run 3.

Table 4
Measured wave parameters using a directional wave rider buoy, estimated parameters as outlined in Section 3, and the estimation error calculated by (13).

Run	Heading	Measurements			Estimates			Estimation errors		
		β[deg]	H_s [m]	T_p [s]	$\hat{\beta}$ [deg]	$\hat{H}_s$ [m]	$\hat{T}_p$ [s]	$\tilde{\beta}$ [deg]	$\tilde{H}_s$ %	$\tilde{T}_p$ %
1	Head	−175.6	2.27	10	−180	2.1044	9.638	4.39	7.56	3.617
1	Beam	95.1	2.27	10	90	2.26	9.638	5.1	0.725	3.167
1	Stern quartering	50	2.27	10	45	1.999	9.781	5	12.16	2.192
1	Following	4.3	2.27	10	0	2.161	9.781	4.3	5.08	2.192
2*	Head	179	1.71	8	180	1.6747	10.48	1	1.846	30.03
2*	Bow quartering	134.8	1.71	8	135	1.8724	8.091	0.2	9.779	1.133
2*	Beam	89.2	1.71	8	90	1.8708	8.402	0.8	9.685	5.02
2*	Stern quartering	44.2	1.71	8	45	1.5834	8.192	0.8	7.165	2.398
2*	Following	−0.3	1.71	8	0	1.821	8.511	0.3	6.760	6.394
3	Head	−171.6	1.925	15.3	−180	1.9451	13.374	8.45	1.03	12.58
3	Beam	−79	1.925	15.3	−90	1.961	13.163	11	1.838	14.33

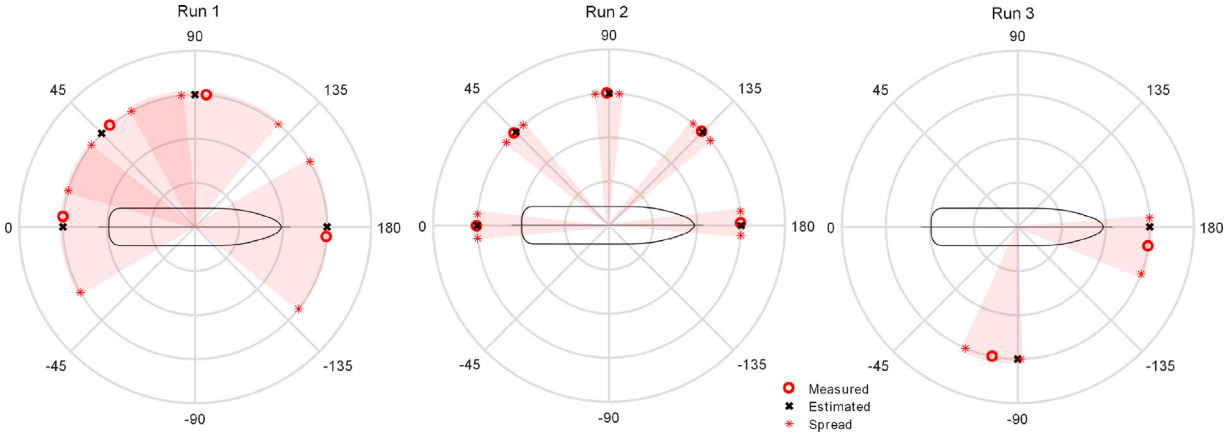

Fig. 12. Measured and estimated relative wave direction β, and $\hat{\beta}$ in [*deg*] for sea states in Runs 1–3. The spread for the sea state in Run 1 is 34°, so the sectors are overlapping for some directions. Keep in mind that the wave propagation direction Θ in the global frame is constant and that the vessel is changing heading.

whereas the pitch peak is single-peaked for all estimates. In Table 4 the estimation errors for Run 2*, i.e., for the alternative formulation of Run 2, are stated. According to the wave measurements, there is almost the same amount of energy around the swell peak frequency as around the wind-generated wave peak frequency. However this is not reflected in the estimated wave parameters $\hat{\beta}$, $\hat{H}_s$ and $\hat{T}_p$, which are all (except $\hat{T}_p$ for head seas) estimating the wind-generated wave.

The largest estimation error for the peak period occurs for the sea state in Run 2 for head seas $\tilde{T}_p = 30.0\%$. Here, the two-peaked heave response has a slightly higher peak corresponding to the swell waves, as can also be seen in Fig. 10. Coincidentally, the significant wave height estimate for the same case is the best for this sea state, with $\tilde{H}_s = 1.85\%$.

The measured relative wave direction and spread, and the estimated relative wave directions are shown in Fig. 12 for all runs. The mean estimation error for the relative wave direction was $\tilde{\beta} = 3.75°$, with a standard deviation of 3.41°. The largest estimation error occurred for Run 3 in beam seas of $\tilde{\beta} = 11°$. However, since the test cases were for $\beta = \{0, 45, 90, 135, 180\}$, and the method is designed to estimate exactly these wave directions, the estimation error $\tilde{\beta}$ is misleading. In general the method identifies a wave direction within 45° intervals, which theoretically gives a maximum estimation error of $\tilde{\beta} = 22.5°$. All relative wave directions in these test cases were identified correctly.

The waves had a relatively large spread in the first sea state of 34°, as seen by the overlapping sectors in Fig. 12. It is not easy to detect which effects (if any) this large spread has had on the estimates. As mentioned, the iteration in (4) does not differentiate between multiple (directional) peaks, but rather makes an indirect energy-directional average, and the procedure outlined in Section 3.2 selects the direction with the best agreement of energy. Therefore the estimated wave direction for the sea state in Run 2 corresponds fairly well for the wind-generated waves, and not at all for the swell.

4.5. General discussion

The procedure for estimating the sea state summarized in Fig. 3 works well for the response measurements of R/V Gunnerus in DP. The method requires little tuning in order to work, and is computationally efficient[3], solving $3 \times N_\beta$ linear equations through iteration. Here 15 minutes of response measurements were used for the response spectra, so having some overlap in the samples, a reliable sea state estimate could be available in a controller every 10 min, if necessary. Other parameters than the significant wave height, peak period and wave direction may be derived as input to control algorithms as well.

The DP control system kept R/V Gunnerus well in position in these data sets, which is a good basis for sea state estimation. As mentioned in Section 2.1, the size of the vessel compared to the waves influences the quality of the sea state estimates. Usually, the control algorithm in DP filters out the wave-frequency vessel motion from the control law so that first-order wave motions are not compensated for. Hence, it is expected that DP will not actuate in the first order range, but in this case there could be some influence on the controlled surge, sway and yaw motion, since the

[3] The execution time for the slowest case was 0.1 s on an Intel(R)Core(TM)i7-4600U CPU @ 2.10 GHz.

vessel is relatively small compared to the waves. This is especially a concern for sea state estimation using the roll motion in beam sea, since the maximum roll angles for this relative wave direction are around 10°, and may hence be influenced by the controlled sway and yaw motions. The maximum pitch angles were generally below 5°, so the couplings between the controlled surge motion, and the heave and pitch motions used for estimation, are thought to be small.

The maximum heading deviation from the setpoint was 5.87°, which occurred in beams seas for Run 3, and the average standard deviation of the heading was 1.30°. These are usual values for heading deviation for moderate sea states, which is the case for the relatively small R/V Gunnerus in the data sets examined here [29]. Since the relative wave direction estimate is an energy-directional average found based on a timeseries of measurements, the influence of small oscillations in heading about the setpoint are thought to be small. The influence of the directional spread of the waves is anticipated to be much more significant. Although not shown, examination of the covariance of the response measurements reveals that the vessel is in steady state for most of the time series. However, in some of the data sets the response is not stationary, so the steady-state assumption may be relaxed.

5. Conclusion

The sea state estimation algorithm presented in this paper was a rather direct/brute-force kind of (spectral) approach which was shown to be computationally efficient. The method required little tuning in order to work, and relied only on the vessel responses and main vessel parameters. The method has proved so far to have good estimating performance, with an average significant wave height estimation error of 5.79%, average peak period estimation error of 7.59%, and the relative wave direction was estimated within the correct 45° interval for every data set. Therefore, the method could stand alone but, due to its high computational efficiency, it might also be used as an 'initial sea state estimator' that gives a starting guess for some of the more established sea state estimation techniques based on Bayesian statistics or parametric optimization, e.g., [6,11,12,28]. The fast estimation capabilities will be promising for improving transient performance of the DP system.

This initial study was particularly relevant for DP (no forward speed), but in the meantime the procedure has been generalized to include advance speed and short-crested waves [30]. For future work, a sensitivity study on the number of samples in the FFT of the vessel responses, and the vessel size compared to the wave length, and a comparative study where the method when using the vessel transfer functions instead of the closed-form expressions should be completed.

Acknowledgements

This work was supported by the Research Council of Norway through the Centres of Excellence funding scheme, project number 223254 NTNU AMOS. The data presented in this paper was collected during sea trials in 2013 in connection with the SIMVAL KPN project (grant number 225141/O70). The data collection was financed by Rolls-Royce Marine and the Norwegian Research Council through grant number 226412/O70. Thanks to Rolls-Royce Marine for permission to publish the results.

References

[1] A.J. Sørensen, A survey of dynamic positioning control systems, Annu. Rev. Control 35 (1) (2011) 123–136.
[2] M. Ludvigsen, A.J. Sørensen, Towards integrated autonomous underwater operations for ocean mapping and monitoring, Annu. Rev. Control 42 (2016) 145–157.
[3] G.F. Clauss, S. Kosleck, D. Testa, Critical situations of vessel operations in short crested seas-forecast and decision support system, J. Offshore Mech. Arctic Eng. 134 (2012), http://dx.doi.org/10.1115/1.4004515.
[4] D.C. Stredulinsky, E.M. Thornhill, Ship motion and wave radar data fusion for shipboard wave measurement, J. Ship Res. 55 (2011) 73–85.
[5] E.M. Thornhill, D.C. Stredulinsky, Real time local sea state measurement using wave radar and ship motions, SNAME Annual Meeting, Seattle, WA, USA (2010).
[6] U.D. Nielsen, Estimations of on-site directional wave spectra from measured ship responses, Mar. Struct. 19 (2006) 33–69.
[7] T. Iseki, K. Ohtsu, Bayesian estimation of directional wave spectra based on ship motions, Control Eng. Pract. 8 (2) (2000) 215–219, http://dx.doi.org/10.1016/S0967-0661(99)00156-2.
[8] R. Pascoal, C. Guedes Soares, Kalman filtering of vessel motions for ocean wave directional spectrum estimation, Ocean Eng. 36 (6–7) (2009) 477–488, http://dx.doi.org/10.1016/j.oceaneng.2009.01.013.
[9] E. Tannuri, J. Sparano, A. Simos, J. Da Cruz, Estimating directional wave spectrum based on stationary ship motion measurements, Appl. Ocean Res. 25 (5) (2003) 243–261, http://dx.doi.org/10.1016/j.apor.2004.01.003.
[10] U.D. Nielsen, A concise account of techniques available for shipboard sea state estimation, Ocean Eng. 129 (2017) 352–362, http://dx.doi.org/10.1016/j.oceaneng.2016.11.035.
[11] C. Møgster, Sea State Estimation Using Bayesian Modeling Methods, Department for Marine Technology, (NTNU), Supervisor: Asgeir J. Sørensen, 2015 (Master's thesis).
[12] T. Iseki, Real-time analysis of higher order ship motion spectrum, ASME, International Conference on Offshore Mechanics and Arctic Engineering, 29th International Conference on Ocean, Offshore and Arctic Engineering 2 (2010) 399–405, http://dx.doi.org/10.1115/OMAE2010-20521.
[13] T.D. Nguyen, A.J. Sørensen, S.T. Tong Quek, Design of hybrid controller for dynamic positioning from calm to extreme sea conditions, Automatica 43 (5) (2007) 768–785.
[14] D.J.W. Belleter, R. Galeazzi, T.I. Fossen, Experimental verification of a global exponential stable nonlinear wave encounter frequency estimator, Ocean Eng. 97 (2015) 48–56, http://dx.doi.org/10.1016/j.oceaneng.2014.12.030.
[15] A.H. Brodtkorb, U.D. Nielsen, A.J. Sørensen, Sea state estimation using model-scale DP measurements, in: MTS/IEEE OCEANS, Washington, DC, 2015.
[16] U.D. Nielsen, M. Bjerregård, R. Galeazzi, T.I. Fossen, New concepts for shipboard sea state estimation, in: MTS/IEEE OCEANS, Washington, DC, 2015.
[17] U.D. Nielsen, A.H. Brodtkorb, J.J. Jensen, Response predictions for marine vessels using observed autocorrelation function, MarStruct 58 (March) (2018) 31–52 https://doi.org/10.1016/j.marstruc.2017.10.012.
[18] J. Jensen, A. Mansour, A. Olsen, Estimation of ship motions using closed-form expressions, Ocean Eng. 31 (2004) 61–85.
[19] WAMIT Inc, WAMIT – State of the art in wave interaction analysis, Massachusetts USA, 2017 http://www.wamit.com.
[20] Sintef Ocean, ShipX, Trondheim, Norway, 2017 http://www.sintef.no/programvare/shipx/.
[21] A. Papanikolaou, E. Boulougouris, D. Spanos, On the roll radius of gyration of ro-ro passenger ships, 7th International Society of Offshore and Polar Engineers (ISOPE) Conference III (1997) 499–507.
[22] J. Hua, M. Palmquist, Wave estimation through ship motion measurement, Technical Report, Naval Architecture, Department of Vehicle Engineering, Royal Institute of Technology (1994).
[23] M. Aschehoug, Scientific paper on the sea state estimation methodology, Technical Report, SIREHNA, France [Paper prepared in the HullMon+ project] (2003).
[24] U.D. Nielsen, Estimation of directional wave spectra from measured ship responses, Section of Coastal, Maritime and Structural Engineering, Department of Mechanical Engineering, Technical University of Denmark, May, 2005 (PhD thesis).
[25] S. Steen, Ø. Selvik, V. Hassani, Experience with rim-driven azimuthing thrusters on the research ship Gunnerus, in: High-Performance Marine Vessels, Cortona, Italy, 2016.
[26] R. Skjetne, K. Kjerstad, S.A.T. Værnø, A.H. Brodtkorb, A.J. Sørensen, M.E.N. Sørensen, M. Breivik, V. Calabrò, B.O. Vinje, AMOS DP research cruise 2016: academic full-scale testing of experimental dynamic positioning control algorithms onboard R/V Gunnerus, in: ASME. International Conference on Ocean, Offshore and Arctic Engineering (OMAE), Trondheim, Norway, 2017.
[27] WAFO-group, WAFO – A Matlab Toolbox for Analysis of Random Waves and Loads – A Tutorial, Math. Stat., Center for Math. Sci., Lund Univ, Lund, Sweden, 2000.
[28] N. Montazeri, U.D. Nielsen, J.J. Jensen, Estimation of wind sea and swell using shipboard measurements – a refined parametric modelling approach, Appl. Ocean Res. 54 (2016) 73–86, http://dx.doi.org/10.1016/j.apor.2015.11.004.
[29] T.I. Fossen, J.P. Strand, Passive nonlinear observer design for ships using Lyapunov methods: full-scale experiments with a supply vessel, Automatica 35 (1) (1999) 3–16.
[30] U.D. Nielsen, A.H. Brodtkorb, A.J. Sørensen, A brute-force spectral approach for wave estimation using measured vessel responses, Mar. Struct. (2017) (submitted for publication).
[31] U.D. Nielsen, Response-based estimation of sea state parameters – influence of filtering, Ocean Eng. 34 (13) (2007) 1797–1810.
[32] U.D. Nielsen, The wave buoy analogy – estimating high frequency wave excitations, Appl. Ocean Res. 30 (2) (2008) 100–106.